



# Journal of Applied and Computational Mechanics



## Research Paper

# Optimization of Spark Ignition Engine Performance using a New Double Intake Manifold: Experimental and Numerical Analysis

Mostafa Khaje Zade Roodi<sup>1</sup>, Ali Jalali<sup>2</sup>, Ali Hedayati<sup>3</sup>, Amin Amiri Delouei<sup>4</sup>

<sup>1</sup> Department of Mechanical Engineering, Payame Noor University (PNU), Tehran, P.O.BOX, 19395,3697, Iran, Email: mostafakhajezadeh@gmail.com

<sup>2</sup> Department of Mechanical Engineering, Payame Noor University (PNU), Tehran, P.O.BOX, 19395,3697, Iran, Email: a\_jalali@pnum.ac.ir

<sup>3</sup> Department of Mechanical Engineering, Ferdowsi University of Mashhad, Mashhad, Iran, Email: ali.hedayati.sa@gmail.com

<sup>4</sup> Department of Mechanical Engineering, University of Bojnord, Bojnord 945 3155111, Iran, Email: a.amiri@ub.ac.ir

Received July 03 2020; Revised November 01 2020; Accepted for publication November 04 2020.

Corresponding author: Amin Amiri Delouei (a.amiri@ub.ac.ir)

© 2021 Published by Shahid Chamran University of Ahvaz

**Abstract.** In this study, the effect of different intake manifold geometries on the performance of a spark-ignited engine is investigated both numerically and experimentally. 1D and 1D-3D simulations are carried out to find the optimal dimensions of different intake manifold designs. The numerical simulations are successfully validated with real data. The results show that the manifold design utilizing two-valve throttle has a better performance. The superior design is constructed and mounted on the engine to compare the output result with the base design. The operation tests are performed at various rotational speeds in the range of 1000-6000 rpm. Regarding the experimental tests, the superior double intake manifold increases the engine brake power and torque by 6.814%.

**Keywords:** Double intake manifold, 1D-3D numerical simulation, Experimental test, Optimization, SI engine.

## 1. Introduction

a mixture of fuel and air is needed to generate power in internal combustion engines. In the intake stroke, the intake valve opens, and the air enters the intake system due to the difference between the cylinder and the ambient pressure and then flows through the intake system to the cylinder. The intake manifold is one of the most effective components of the engine suction system [1,2]. The intake manifold in spark-ignited engines is connected to the throttle and the intake ports (runners) of the cylinder head. By changing the angle of the throttle, the inlet air to the engine is controlled and distributed through the intake manifolds between the cylinders. Important criteria for intake manifold design are: low resistance to airflow, proper distribution of fuel and air between cylinders, proper length of ducts and branches to take advantage of the effects of RAM, use of flow momentum entering the cylinder to continue suction flow to the cylinder is called RAM, and sufficient heating to ensure fuel evaporates in the Carburetor spray engines or engines with a spray-on throttle. In intake manifold design, some important considerations are required; for example, the size of ducts and branches should be large enough to allow sufficient airflow to transport the fuel droplets. To take advantage of the RAM effect, equal branches of larger and longer ducts and bends with larger bending angles are used [1]. In the following, some of the research carried out in the field of intake manifolds are discussed:

Keoleian and Kar [2] Studied 3D intake manifolds and analyzed their design parameters using the cycle design method. The results showed that nylon composite manifold reduces fuel consumption, but it increases the cost of production. Siqueira et al. [3] simulated an inlet manifold to investigate the pressure distribution in each of the four inlet pipes in different engine performance cycles. By comparing three different types of the plenum, they were looking for the best engine performance. After simulating the flow, they observed that the transient analysis yields more realistic results than the steady flow analysis, but the major disadvantage of this analysis is the time it takes and the need for the correct boundary conditions to be solved accurately. Ceviz [4] conducted a basic study on the influence of intake plenum geometry on performance of an engine. The results indicate that the intake plenum volume has a great influence on the studied parameters. Also, a new intake manifold for a spark-ignited engine is developed by Ceviz and Akin [5]. This new manifold design is equipped with variable length plenum. The results show more fuel consumption at high load and low engine rotational speeds. Jemni et al. [6] worked on a three-dimensional numerical simulation of the turbulent flow through the two manifolds. The proposed model was based on solving Navier-Stokes and energy equations by the help of the three-dimensional CFD code. The results show that brake power, brake torque, and brake thermal efficiency are improved by 16%, 13.9%, and 12.5%, respectively. A new technique for online estimation of throttle valve's discharge coefficient is developed by Butt et al. [7]. Vichi et al. [8] worked on an engine intake system with variable geometry. They tried to optimize engine power and vehicle drivability. The proposed optimal plenum volume to enhance engine performance. Manmadhachary et al. [9] designed a diesel engine's spiral intake manifold to enhance volumetric efficiency. They concluded that



the size and shape of the manifold has a significant effect on volumetric engine efficiency. Direct numerical simulation is used by Giannakopoulos et al. [10] to study the incompressible flow in the intake pipes of a manifold. They investigate the effect of boundary conditions on flow physics. Zhao et al. [11] used the GT-Power software to investigate the effect of variable valve timing and cylinder-deactivation in a 4-cylinder SI engine manifold. They showed that their strategy could improve the fuel economy of the SI engine. Also, Hall et al. [12] work on modeling SI engines with variable valve timing. Silva et al. [13] numerically studied the optimal length of runners in the intake manifold of a 4-cylinder SI engine. The GT-Power software is used for their 1D simulations. They claimed that the optimal runner length is shorter in the high engine rotational speed and will increase with a decrease of engine rotational speed. Three new intake manifold designs for a single-cylinder diesel engine are presented by Sadeq et al. [14]. Spiral-helical geometries with different helical diameter are used in this study. The detailed effects of manifold geometry and fuel properties on engine emission are reported simultaneously. Souza et al. [15] performed a numerical investigation on a 4-stroke Otto engine with one intake valve per each of four cylinders. The GT-Power software package is utilized for one-dimensional numerical simulations. The influence of manifold geometry on engine efficiency is the main target of this study. An experimental setup is comprised of an Otto engine driven by an electrical motor. Souza et al. [15] show that their new manifold geometry can improve engine efficiency by 6%. Liu et al. [16] investigated the characteristics of alcohol/kerosene as fuel for aero spark-ignition engine. the results show that this kind of fuel (alcohol ratio  $\geq 50\%$ ) can lead to higher efficiency than gasoline. Menzel et al. [17] conducted a multi-objective optimization to find maximum volumetric and thermal efficiency of the internal combustion engine. The considered design variables in their study were inlet and exhaust valves timing. Mariani et al. [18] using an extreme learning machine to study the cyclic of a spark-ignition engine. the results show that the mean effective pressure obtained by this method is in good agreement with the experimental data and ELM leads to better results than other existed technique. Zhao et al. [19] introduced a new ignition strategy using multi-channel sparks. The experimental data indicate that the three-channel sparks raise the ignition probability and extend the fuel-lean ignition limits in comparison with the single-channel discharge. Och et al. [20] utilized a mathematical optimization procedure to improve the gas exchange process of a single-cylinder ignition engine. the considered optimization variables were duct lengths and valve timing. Also, the objective function was the volumetric efficiency. The results showed that optimal valve timing increases the volumetric efficiency. Shi et al. [21] simulated the intake manifold of a spark-ignition Wankel engine. the results showed that the ignitability improves in the H<sub>2</sub>-enriched ignition environment. Gocmen et al. [22] studied the solutions of reducing the pressure drop in a compression ignition engine. Actually, by simulating the intake manifold of a diesel engine in Ansys-Fluent software, they decided to find a plan to reduce the pressure drop in the intake manifold. The pressure drop reduction leads to reduce the pressure difference between the inlet and outlet of the manifold. The main purpose of their study is to achieve an ideal design of the intake manifold that distributes the inlet flow between the cylinders equally. Their results show that the proposed manifold model has a significant effect on reducing the flow pressure drop.

Improving the performance of internal combustion engines and controlling their pollutant emissions are one of the most important goals of engine development engineers. The purpose of this research is to increase the maximum power and torque of the engine at different rotational speeds by designing and constructing a superior intake manifold. Increasing the power and torque of the engine allows the vehicle to reach maximum rotational speed in a shorter time. In the present study, both 1D and 1D-3D simulations are utilized. Both of these numerical simulations are achieved based on the optimal dimensions using the GT-Power simulation platform. The objective function in the present optimization is to increase the torque and power of the engine. Of course, the optimum manifold must be mountable on the engine due to location restrictions. At the same time, the manufacturing process should be as inexpensive and straightforward as possible. The process of doing the research is described in Fig. 1. The superior intake manifold design is manufactured by manual molding of epoxy with glass fibers. The superior manufactured manifold is mounted on the engine, and its output torque and power are compared with the same engine equipped with a base manifold. The results show that the proposed superior design can improve engine performance by up to 6.814%.

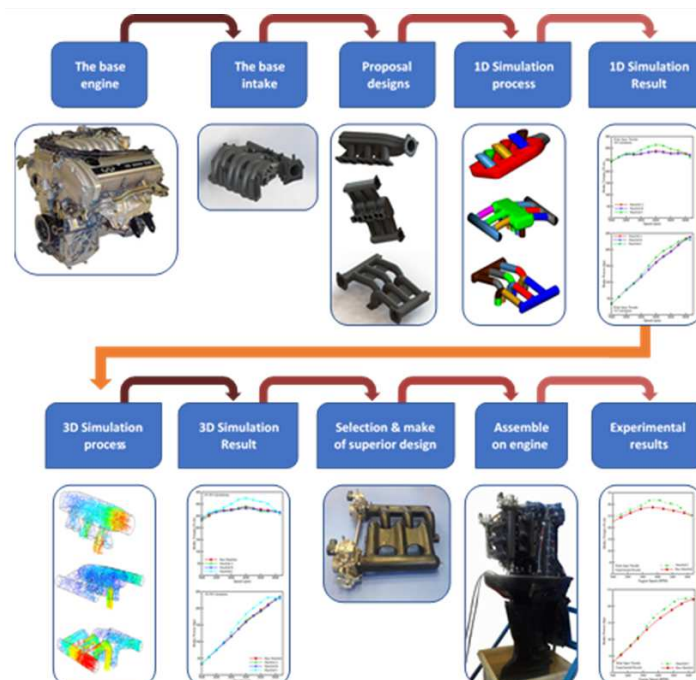


Fig. 1. The process of turning an idea into a product in this study.



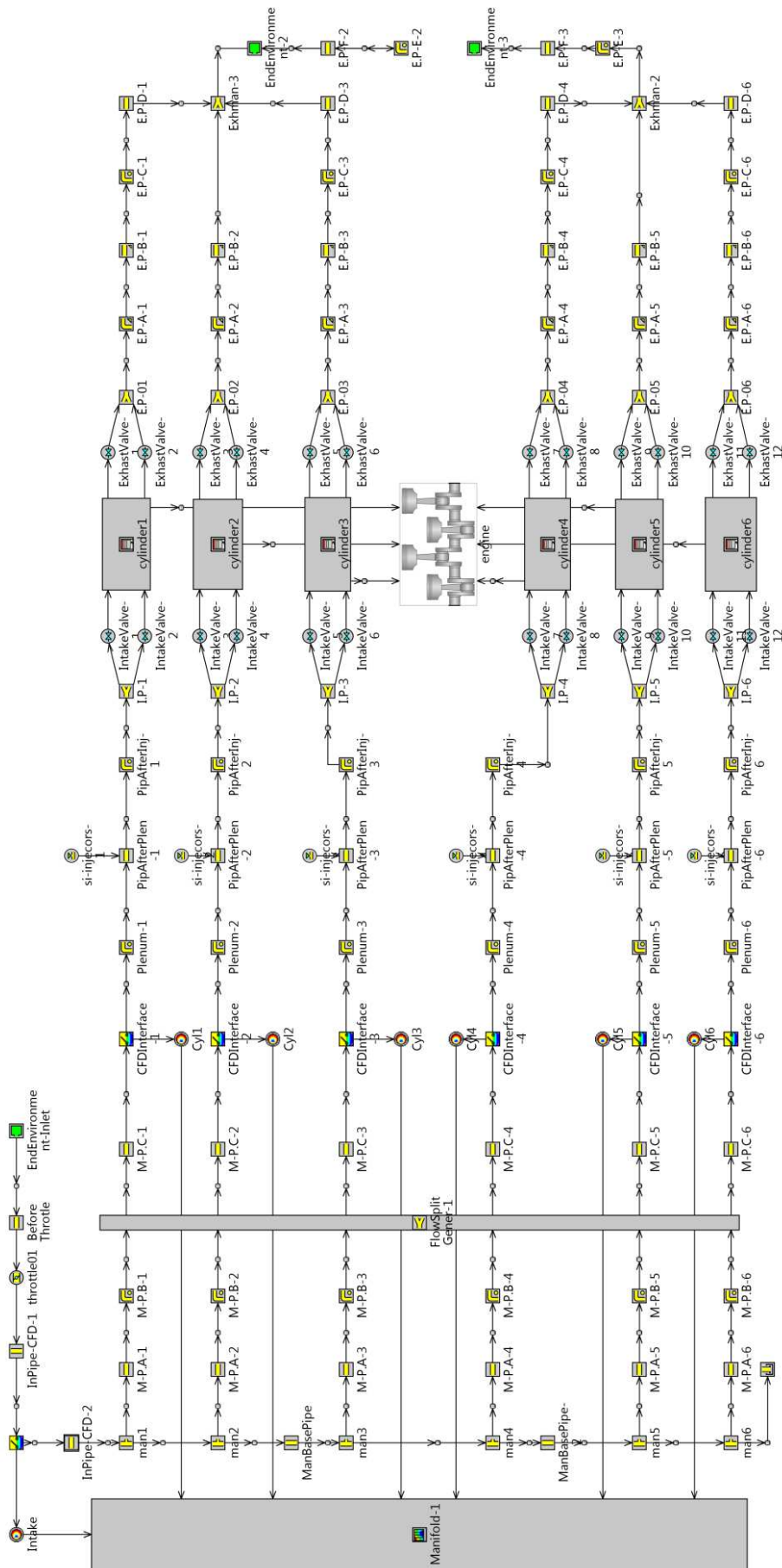


Fig. 2. Model used to simulate the flow in the base engine.



**Table 1.** General specifications of the base engine

Parameter	Specification
No. Cylinder	6 cylinder, V type, SI gasoline, 4-stroke
Type of cooling	Water-cooled Engine
Bore (m)	0.093
Stroke (m)	0.073
Max. Power (HP)	230
Capacity, cc/compression ratio	2988/10
Maximum rotational Speed (rpm)	6200
Intel Valve Opens (deg)	3 BTDC
Intel Valve Closes (deg)	139 BTDC
Exhaust Valve Opens (deg)	49 BBDB
Exhaust Valve Closes (deg)	3 ATDC

**Table 2.** Main properties of the pure fuel used

Properties	Gasoline
Approx. formula	C <sub>8</sub> H <sub>18</sub>
Density at 15 °C (kg/m <sup>3</sup> )	734
Octane number. engine	91-94
Calorific value(kJ/kg)	43400
Molecular weight vapor pressure (kPa) at 38°C	100
Boiling point (°C)	62-90
Enthalpy of vaporization (kJ/kg). at 298 k	310
Lower heating value mass (MJ/kg)	44.5
Lower heating value volume (MJ/l)	32.9
Lambda	0.94-1.04
Conditioning temperature (K)	298
Adiabatic flame temperature (K)	2266

## 2. Numerical Simulation of the Base Engine

### 2.1 Engine specifications

Before the numerical simulating of the engine, it is necessary to investigate the engine specifications discussed in the present study. The specifications of this engine are shown in table 1. Also, the main properties of pure fuel are presented in table 2.

### 2.2 One-dimensional simulation of the base engine

In the present study, a one-dimensional simulation of engine performance is performed with the GT-Power software package, which is widely used in internal combustion engine studies [11, 13, 15, 23-31]. This software is appropriate to simulate engine power circuit, but due to the need for much input information for the simulation, the simulation process will have some difficulties. In this case, experimental data is needed to minimize the error in the simulation process. Some of the experimental data needed in the one-dimensional simulation process require engine performance tests, which can be economically costly to perform above tests. To simulate the engine power circuit in the GT-Power software, each of the engine components such as inlet, and outlet pipes, throttle, fuel sprinkler, intake, and outlet manifolds, intake, and exhaust valves, cylinders, pistons, and crankshaft must be defined in the software. After geometric measurements of the components' dimensions involved in the simulation process as well as measurements of engine performance variables such as opening, and closing timing of engine valves, spark plugs, inlet air temperature to the engine, etc., a one-dimensional engine power generation system for the base engine will be as Fig. 2. To investigate the accuracy of this numerical model, engine simulation results are compared with the experimental data (Fig. 3). According to Fig. 3, the brake power obtained from engine simulation has an acceptable agreement with the experimental results.

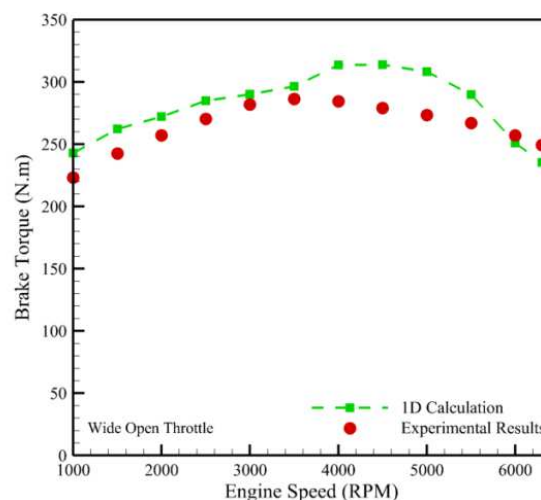


**Fig. 3.** Comparison of brake torque values in 1D simulation and experimental data for the base engine.



### 2.3 Basic fluid flow equations in GT Power software

In the GT power software, the following equations are considered:

$$\frac{dm}{dt} = \sum_{boundaries} \dot{m} \quad (1)$$

$$\frac{d(m_e)}{dt} = -p \frac{dv}{dt} + \sum_{boundaries} (\dot{m}H) - hA_s(T_{fluid} - T_{wall}) \quad (2)$$

$$\frac{d(\rho HV)}{dt} = \sum_{boundaries} (\dot{m}H) + V \frac{dp}{dt} - hA_s(T_{fluid} - T_{wall}) \quad (3)$$

$$\frac{d(\dot{m})}{dt} = \frac{dpA}{dx} + \sum_{boundaries} (\dot{m}u) + \frac{4C_f}{2} \frac{\rho u |u|}{D} \frac{dxA}{dx} - C_p \left( \frac{1}{2} \rho u |u| \right) A \quad (4)$$

where  $m$ ,  $p$ ,  $H$ ,  $T$ ,  $\rho$ ,  $u$ , and  $C_p$  indicate mass, pressure, enthalpy, temperature, density, and specific heat coefficient, respectively. Also,  $h$  and  $A$  are convective coefficient, and heat transfer area, respectively. Equations (1) to (4) are the mass continuity, energy, enthalpy, and momentum equations, respectively. The governing equations for the fluid flow are solved by integrating respect to time and space. This integration can be done both explicitly and implicitly. In the present study, an explicit method has been used to solve the fluid flow field. In this method, the values of pressure, temperature, and other variables in each cell are calculated according to the known values of neighboring cells at each time step. In the present study, for one-dimensional simulation, the pressure and inlet conditions of the suction system and also the outlet of the discharge system are required. The pressure and temperature values for the inlet air are 1 atm, and 293.15 K, respectively. On the other hand, the pressure of the exhaust gases is considered equal to 1 atm.

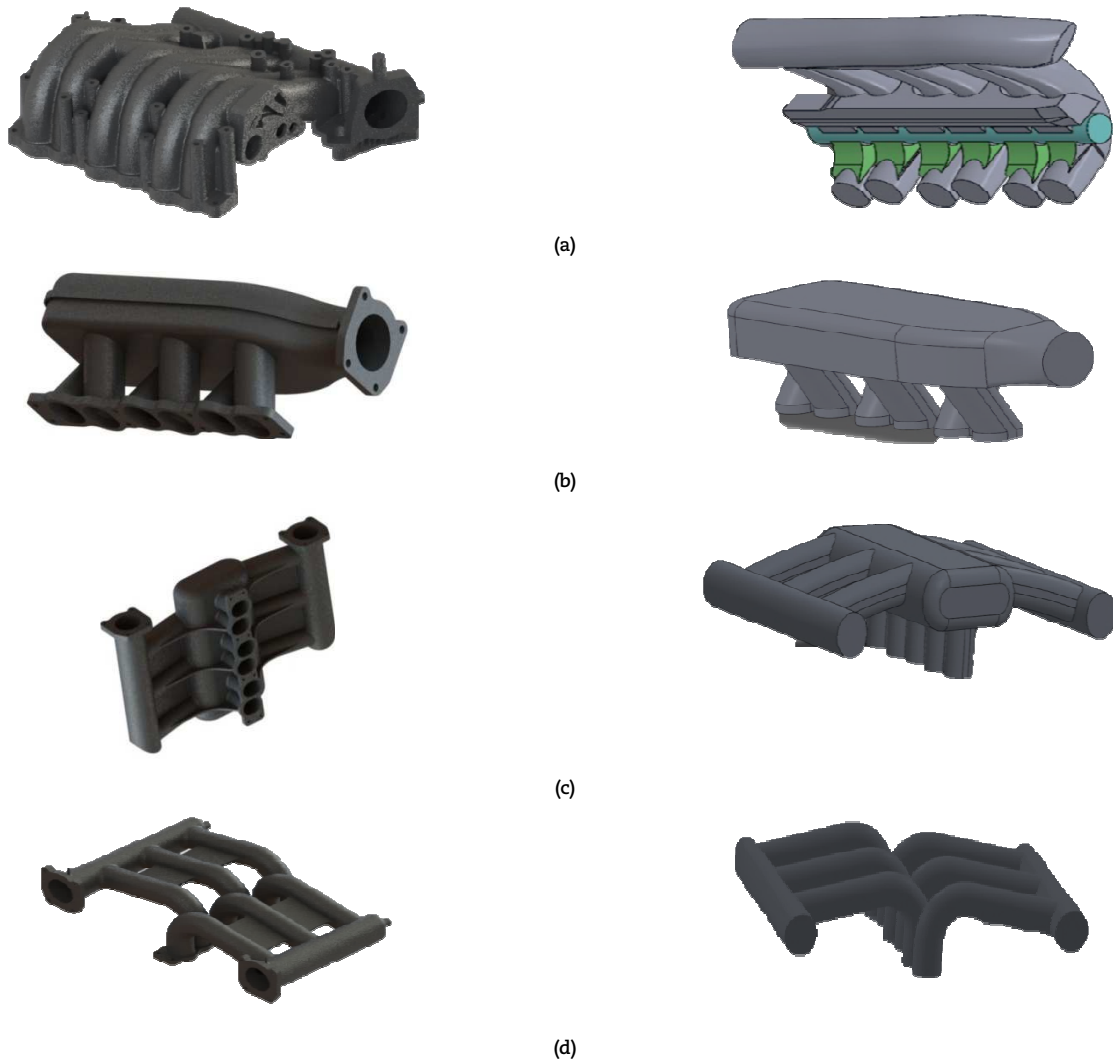


Fig. 4. Proposed designs of intake manifold design of (a) base, (b) type 'A', (c) type 'B', and (d) type 'C'.





**Table 3.** Dimensional optimization range of different intake manifolds for maximum engine brake power and torque

	Runners diameter (mm)	Runners Length (mm)	Sub-plenum volume (10 <sup>3</sup> mm <sup>3</sup> )	Main plenum volume (10 <sup>3</sup> mm <sup>3</sup> )
Manifold design A	40-50	200-300	-	1400-1600
Manifold design B	40-50	200-300	400-600	1400-1600
Manifold design C	40-50	200-300	-	600-800

**Table 4.** Optimal intake manifolds' dimensions for maximum engine brake power and torque

	Runners diameter (mm)	Runners Length (mm)	Sub-plenum volume (10 <sup>3</sup> mm <sup>3</sup> )	Main plenum volume (10 <sup>3</sup> mm <sup>3</sup> )
Manifold design A	40.5	250	-	1600
Manifold design B	42	270	575	1600
Manifold design C	42	275	-	800

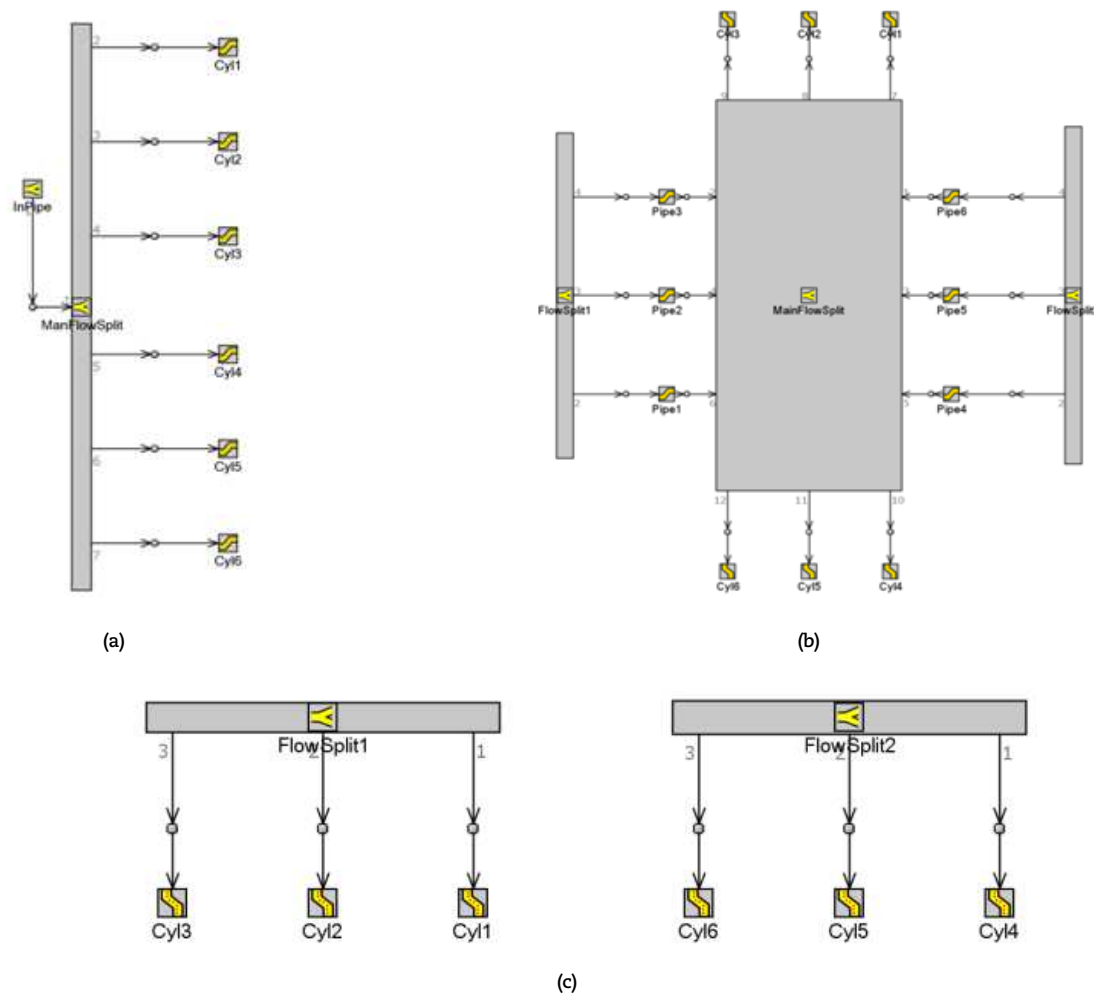
### 3. Numerical Simulation of Samples and Selection of Superior Design

#### 3.1 Suggested geometries

Three designs were considered to improve the maximum power and torque output of the engine. Proposed designs are suggested based on the intake manifold geometry of modern spark-ignited engines as well as creative innovations in using existing designs and combining their design ideas. Concerning the limitations in layout, the availability of raw materials, the manufacturing process, manufacturing costs, and other factors, it results that there are not many plans to consider. The suggested geometries and the basic intake manifold geometry, along with the internal volume of these geometries, are shown in Fig. 4. The proposed intake manifold design must be mounted at the intended location, and also it should be manufactured with acceptable cost. Among the proposed designs, the best design will be selected for construction according to the 1D-3D simulation results.

#### 3.2 One-dimensional simulation and optimization of samples

Regarding the different intake manifolds designs, three different models are considered in the GT-Power software for complete engine simulation (Fig. 5). The optimization process of intake manifold's geometry includes finding the optimal dimensions for maximum power and torque. The dimensional optimization range for maximum engine brake power and torque of proposed manifold designs of 'A', 'B' and 'C' is shown in table 3. The optimal dimensions for maximum engine brake power and torque are obtained by GT-power software. These dimensions are shown in table 4.

**Fig. 5.** 1D models for the manifold design of (a) type 'A', (b) type 'B', and (c) type 'C' in GT-Power software.

After selecting the dimensions introduced in table 4, the engine is re-simulated with the optimized manifolds to determine the brake power and torque at various rotational speeds for different proposed manifolds. Fig. 6 compares engine brake power and torque variations for the engine with different manifolds and the engine with the base manifold. Regarding this figure, one-dimensional simulation implies that the manifold design 'C' has higher brake power and torque over a wide range of engine rotational speeds. By examining the results of the 1D-3D simulation, one can make a more precise decision to choose the best manifold design out of the three proposed designs.

### 3.3 1D-3D simulation

In complex geometry, the results of the 1D simulation may not be accurate enough. To be sure, the 1D-3D simulation can be utilized to improve simulation accuracy. In this method, all engine components are first simulated in 1D, then 3D simulation is performed using 1D information (boundary and initial conditions). For the next step, the results of the 3D simulation is introduced to the 1D solver again. This process is repeated until an engine cycle is completed. Then, in the case of convergence, the solution ends. In the case of non-convergence, the 1D-3D simulation solution will continue. At least 5 to 10, 1D-3D simulation cycles should be performed to reach the acceptable convergence. The 3D solver needs the initial values such as velocity, temperature and species to begin solving the equations of flow in the input path. In the present study, the initial values of velocity and temperature are 0 m/s and 297 K, respectively. The initial values of the species are reported in Table 5. Fig. 7 shows the results of 1D and 1D-3D simulations of the base engine compared to the experimental data. As can be seen, 1D-3D simulation is more accurate than 1D simulation in predicting engine torque variations. It should be noted that both of the simulations are in good agreement with experimental results. However, 1D-3D simulation is more accurate than 1D simulation in predicting changes in engine power and braking torque.

### 3.4 Volumetric efficiency

The intake manifold directly affects engine performance by its influence on the suction process. Fig. 8 shows the changes in volumetric efficiency at different engine performance speeds for different designs of intake manifolds. As can be seen, at low rotational speeds, the volumetric efficiency of the different intake manifold is approximately the same, but after the speed of 2000 rpm, the difference in the volumetric efficiency of the manifold will intensify. According to Fig. 8, the manifold design 'C' has the highest volumetric efficiency after 2000 rpm.

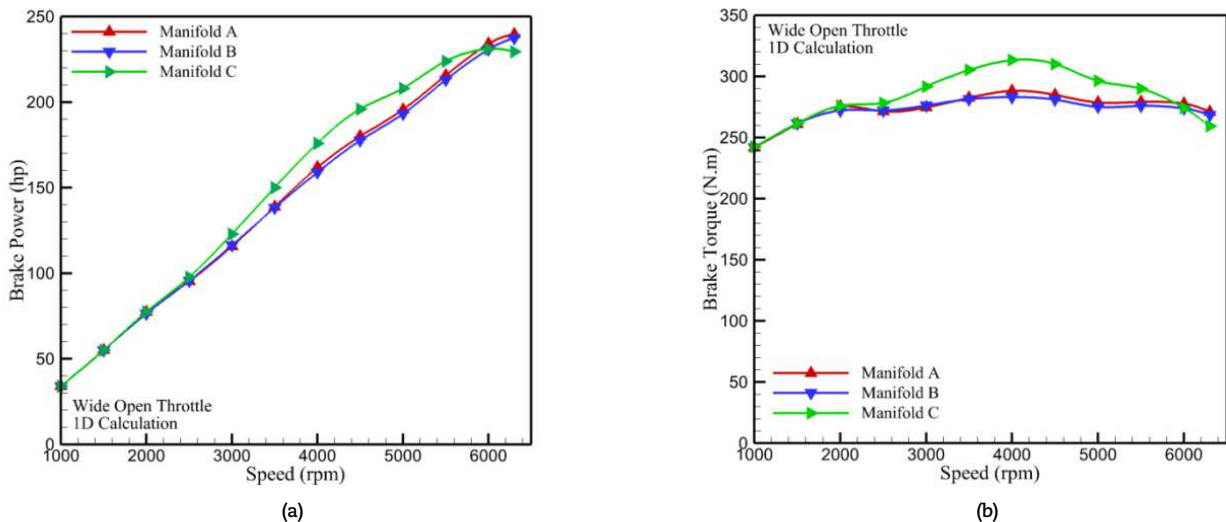


Fig. 6. Variations in (a) brake power and (b) brake torque at different rotational speeds at optimal dimensions.

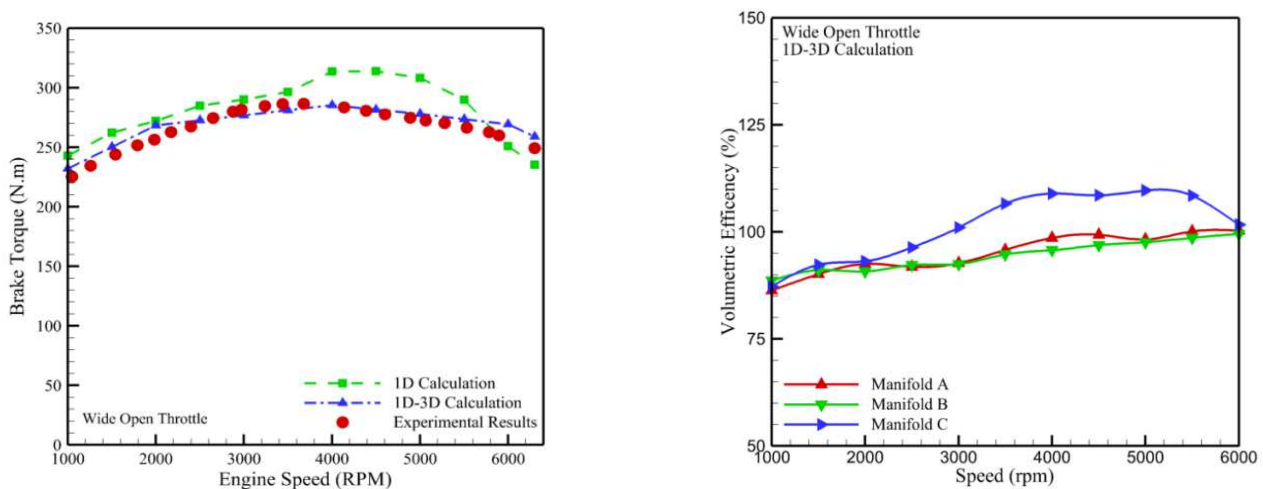


Fig. 7. Comparison of brake torque values of 1D, 1D-3D numerical simulation and experimental data for the base engine.

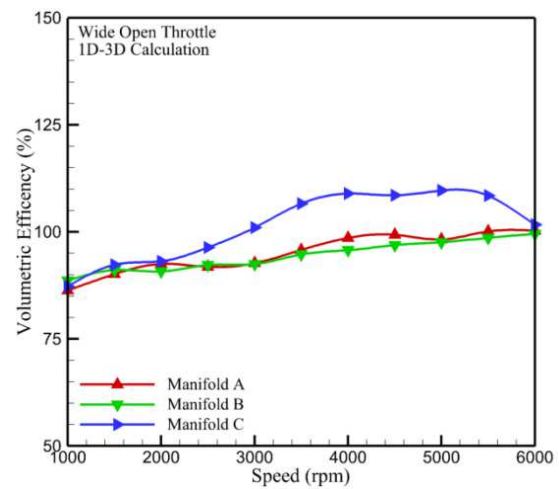


Fig. 8. Comparison of volumetric efficiency variations of 1D-3D numerical simulation at different engine rotational speeds for proposed designs.



**Table 5.** Initial values of species in 3D solver

species	Mass percentage
O <sub>2</sub>	0.018
H <sub>2</sub> O	0.02
CO <sub>2</sub>	0.04
N <sub>2</sub>	0.76

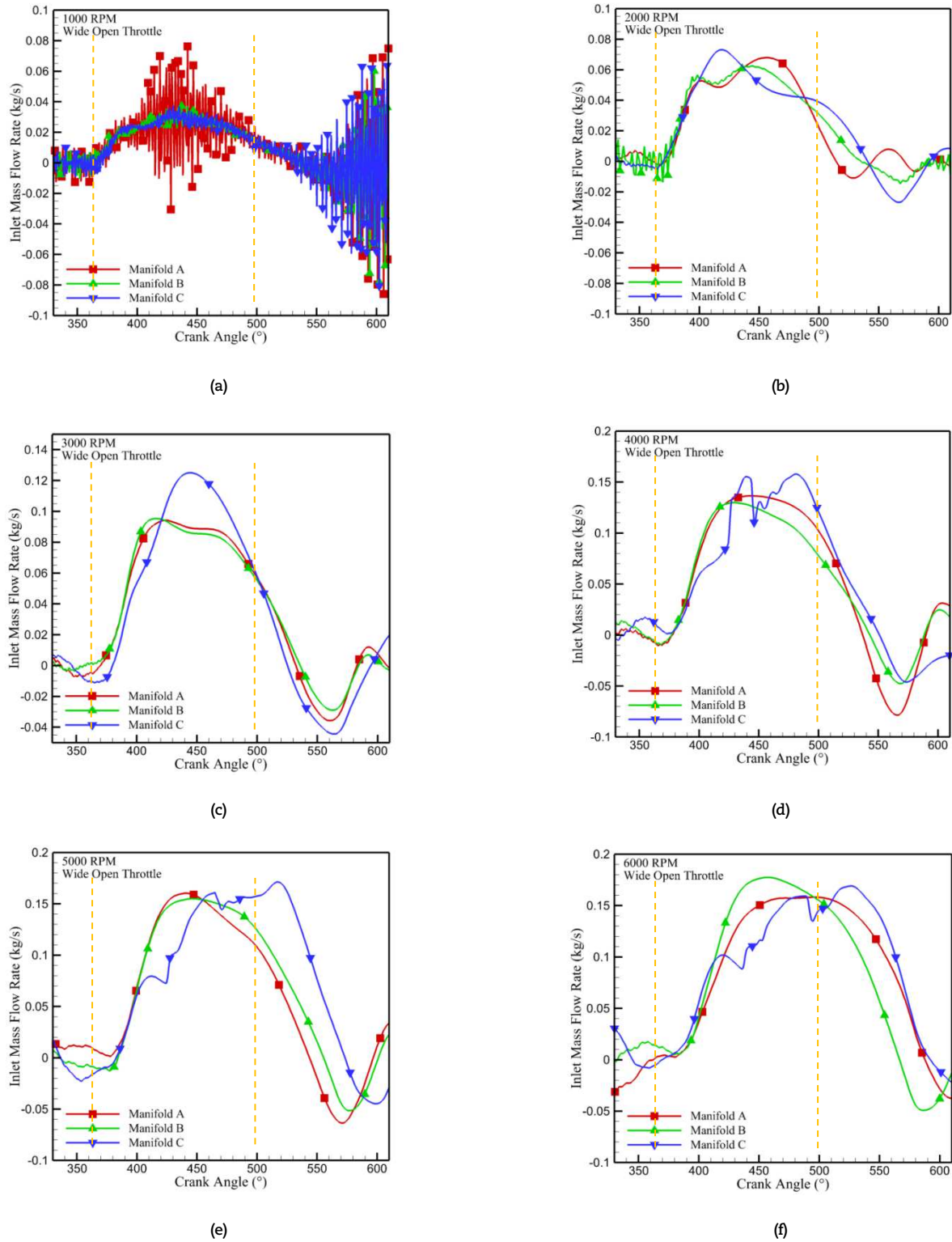


Fig. 9. Mass flow rate variations of air intake to the engine at rotational speeds of (a) 1000 rpm, (b) 2000 rpm, (c) 3000 rpm, (d) 4000 rpm, (e) 5000 rpm, and (f) 6000 rpm. (The opening and closing time of the inlet valve is shown by two dash lines)





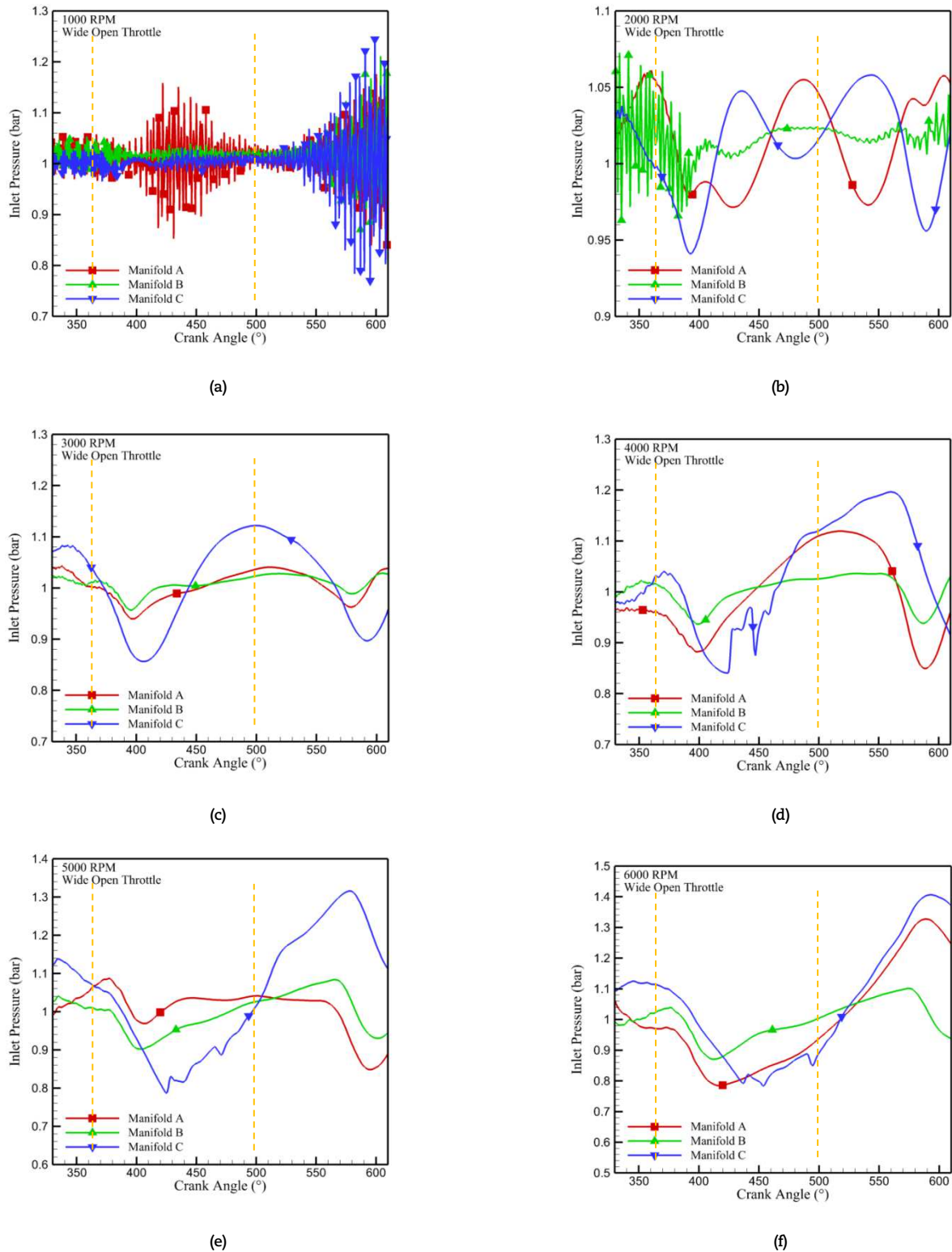


Fig. 10. Pressure variations of air intake to the engine at rotational speeds of (a) 1000 rpm, (b) 2000 rpm, (c) 3000 rpm, (d) 4000 rpm, (e) 5000 rpm, and (f) 6000 rpm. (The opening and closing time of the inlet valve is shown by two dash lines)

The variation in the inlet mass flow rate to the cylinder can result in volumetric efficiency variation and should be analyzed. Fig. 9 shows the mass flow rate variations of the inlet air to the engine for different intake manifold designs. The cylinder pressure varies during the intake stroke (Fig. 10). When the cylinder is suctioned at low engine rotational speeds, the pressure inside the cylinder is first lowered and lead to moving the flow through the manifold to the cylinder. As the pressure difference between the cylinder and the manifold at low rotational speeds is negligible, the cylinder pressure approaches the manifold pressure very rapidly and the flow is reversed. At this moment, the flow goes out of the cylinder. The process of inflow and outflow from the cylinder is repeated until the end of the suction period and the inlet flow fluctuates during the time. This phenomenon is quite evident at rotational speed of 1000 rpm for manifold design A (Fig. 9a). For the manifold designs 'B' and 'C', the flow velocity is higher at the start of suction in the cylinder, and consequently, the pressure drop created at the manifold is



greater (Fig. 9a). For this reason, the flow fluctuations are less observed at manifold designs of 'B' and 'C'. At 2000 and 3000 rpm, the flow fluctuations are noticeably reduced or not observed at all (Fig. 9b and Fig. 9c). Due to the increase in the pressure drop of the cylinder, the flow over the suction process is able to fill the cylinder at a larger interval in the higher speed of the piston movement (Figs. 9b and 9c). For this reason, the flow in the intake stroke of the engine will not oscillate during suction. In the experimental test, the opening and closing times of the valve is set to maximize the engine's volumetric efficiency at near the rotational speed of 4500 rpm. For this reason, the volumetric efficiency in this speed range is maximized in all the proposed manifolds. Subsequently, at 5000 and 6400 rotational speeds, due to the high flow return at the start of suction (owing to the high pressure of the cylinder at the start of the valve opening), a large part of the flowing mass departed from the suction system and the cylinder volume efficiency will decrease. (Figs. 9 and 10). The pressure distribution in the different intake manifolds at rotational speeds of 1000, 4000 and 6000 rpm are shown in Fig. 11. As is evident in all of these figures (Figs. 11a, 10b, and 10c), the presence of an intake plenum in the manifold brings the inlet pressure close to the atmospheric pressure. For example, at intake manifold designs 'A' and 'B', which have relatively large intake plenum, the inside pressure at different rotational speeds is closer to atmospheric pressure (Fig. 11a and 11b). Of course, a large intake plenum is not always a viable solution to improve engine efficiency. Engine intake plenum volume should be proportional to engine requirements. Expanding the intake plenum reduces the flow rate. As the flow velocity decreases at the inlet, the movement of the flow through the inlet to the cylinder will be slower. As the piston speed increases, the velocity of airflow into the cylinder increases too. Increasing the velocity of the inlet air to the cylinder will reduce the pressure in the intake manifold (Fig. 11). Due to the high temperature variations in the runners, especially for type 'C', the thermal stress will be important in selecting of their materials.

### 3.5 Brake power and torque

The variations of brake power and torque at various engine rotational speeds for different intake manifolds are shown in Fig. 12. Regarding this figure, the manifold design 'C' has the highest brake power and torque at various engine rotational speeds. The reasons for the superiority of design C are:

I) Use two standalone intake plenums for six cylinders:

One of the most important advantages of design 'C' is the separation of the inlet flow into two isolated parts. The use of two independent plenums, each controlled by a separate throttle, reduces engine pump losses and optimizes pulse flow. On the other hand, the independence of the manifold plenums makes the fluid flow more regular when it enters the manifold. Using a common plenum to store the entire inlet flow to the manifolds reduces the flow in the intake stroke, thereby reducing volumetric engine efficiency.

II) Reduction of minor losses:

In design 'C', because of two independent throttles, high diameter runners, and low bends, the minor losses are reduced, and consequently, engine pump losses are reduced. The lower pump losses lead to higher fuel conversion efficiency.

III) Increase of RAM effect:

Runners are longer in design 'C' and, as mentioned earlier, it can increase the positive effect of RAM.

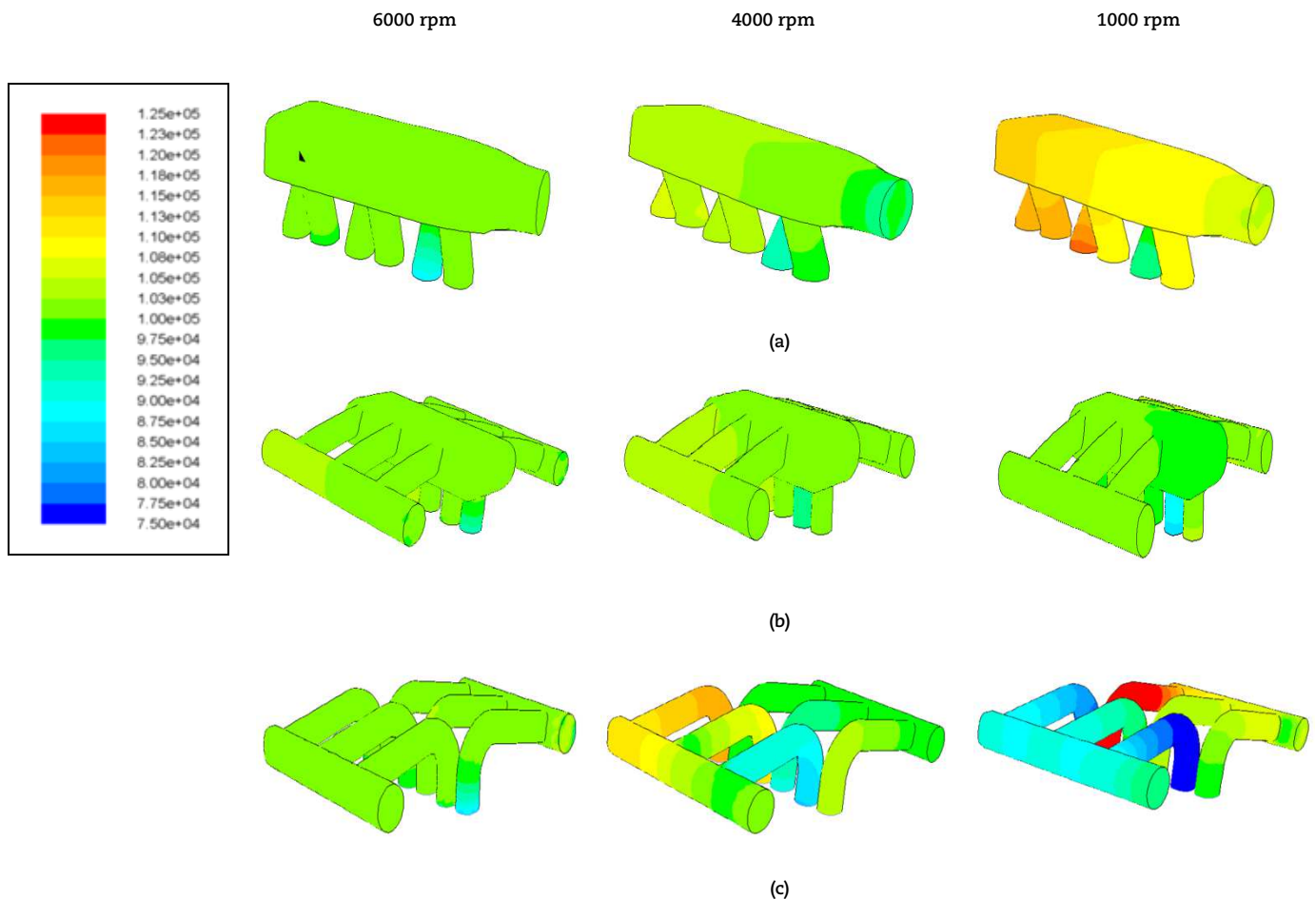


Fig. 11. Absolute pressure distribution in intake manifold design of (a) type A, (b) type B, and (c) type C at different engine rotational speeds

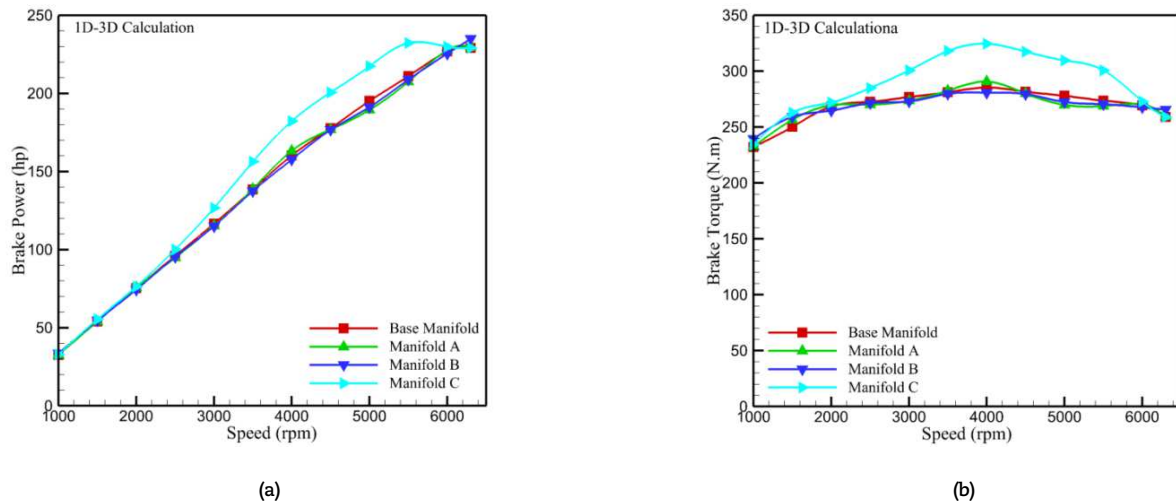


Fig. 12. Variations in (a) brake power and (b) brake torque at different engine rotational speeds.



Fig. 13. Optimal manufactured double intake manifold.

## 4. Manufacture and Experimental Test of the Superior Manifold

### 4.1 Manufacture of the superior manifold

After performing the 1D-3D simulation, the superior manifold design is manufactured to compare with the base one. Fig. 13 shows the superior manifold made by manual molding of epoxy with glass fibers.

### 4.2 Investigation of experimental parameters

Tests were carried out first on the base engine and then on the engine equipped with the superior manufactured manifold. To be sure, the experiments were repeated in three steps, and finally, the mean values were reported. To ensure the proper performance of the engine, the superior manifold is carefully mounted and sealed. During the tests, engine rotational speed is in the range of 1000-6300 rpm with 500 rpm intervals. Also, the throttle is wide open to maximize engine power.

All experiments were performed under the same ambient conditions (table 6). Also, the specifications of the measuring instruments are reported in table 7.

### 4.3 Experimental results of brake power and torque

In the next step, it is necessary to install the manufactured manifold on the engine and compare it with the base manifold.

Firstly, the results of brake power and torque obtained from numerical simulation and experimental test for intake manifold 'C' are compared in Fig. 14a and Fig. 14b, respectively. Regarding Fig. 14, 1D-3D simulation has been able to predict engine power and torque related to intake manifold 'C' to an acceptable level. It should be noted that part of the error in predicting engine brake power and torque is related to the assumptions intended for manifold simulation. For example, the coefficient of friction coefficient is assumed to be the same at different points, while it is not uniform.

Table 6. Laboratory Conditions of the test site.

City	Sea level (m)	Air pressure (bar)	Air temperature (°C)	Relative humidity
Mashhad, Iran	986	0.89	25	15%

Table 7. Specifications of measuring instruments.

Parameter	Measuring instruments	Accuracy
Engine rotational speed	Pickup speed sensor	10 RPM
Engine torque	Hydraulic dynamometer, torque meter	1 N.m
Engine power	Corresponding mathematical relations	0.5 hp



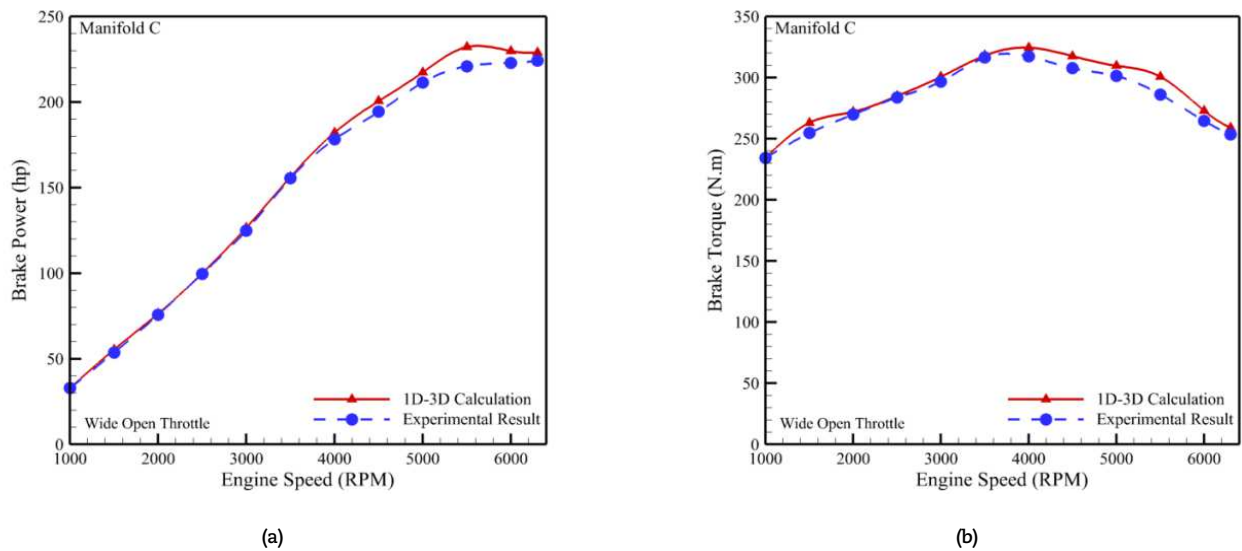


Fig. 14. Comparison of experimental values and numerical simulation results of (a) brake power and (b) brake torque at different engine rotational speeds.

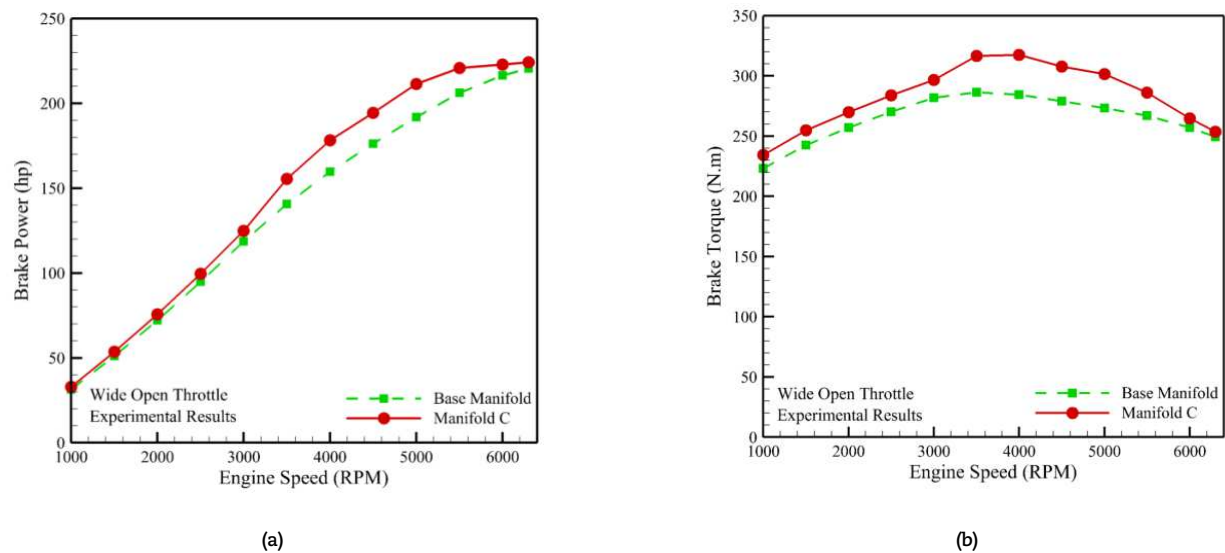


Fig. 15. Comparison of the experimental values of (a) brake power and (b) brake torque at different engine rotational speeds in the basic manifold and designed manifold 'C'.

In the end, the experimental output of the engine brake power and torque obtained from the engine test for two types of manifolds (base and optimal) are compared. Fig. 15 shows the experimental values of engine brake power and torque at various rotational speeds for base manifold and designed manifold 'C'. Regarding Fig. 15, intake manifold design 'C' has been able to increase engine brake power and torque by an average of 6.814%. According to the results, it can be concluded that the manifold design 'C' has been capable of increasing the brake power and torque of the engine impressively, especially at higher than average values of engine rotational speeds.

## 5. Conclusion

In the present study, the impact of different optimal intake manifold designs on the performance of a 4-stroke SI engine was investigated. For this reason, both numerical calculation and experimental tests are involved. The numerical simulation is validated by real data of the engine output. The most important results obtained in the present study are:

- To improve the engine brake power, it is very effective to use a manifold that reduces the minor losses of the suction path. Increasing the diameter of the runners, considering bends greater than 90 degrees, and utilizing two-valve throttle are essential factors in reducing minor losses in the suction path.
- Increasing the length of the runners can increase the maximum engine torque to some extent. It should be noted that an excessive increase in the runner's length will significantly reduce the maximum engine power.
- Numerical simulations indicate that the 1D-3D simulation has an excellent ability to simulate manifold's flow.
- Comparison of experimental data of the engine equipped with the proposed double intake manifold and the base ones shows that the proposed manifold design can increase engine efficiency by 6.814%. Regarding the costs incurred, this increase in power and torque is noteworthy.





## Author Contributions

Mostafa Khajezadeh Roodi initiated the project, conducted the experiments; Ali Jalali suggested the experiments and analyzed the empirical results; Ali Hedayati developed the numerical modeling and validated the results; Amin Amiri Delouei analyzed the numerical and empirical results. The manuscript was written through the contribution of all authors. All authors discussed the results, reviewed, and approved the final version of the manuscript.

## Acknowledgments

Not applicable.

## Conflict of Interest

The authors declared no potential conflicts of interest with respect to the research, authorship, and publication of this article.

## Funding

The authors received no financial support for the research, authorship, and publication of this article.

## Data Availability Statements

The datasets generated and/or analyzed during the current study are available from the corresponding author on reasonable request.

## References

- [1] Heywood, J.B., *Internal combustion engine fundamentals*, 2<sup>th</sup> ed., McGraw-Hill Inc., 2018.
- [2] Keoleian, G.A., Kar, K., Elucidating complex design and management tradeoffs through life cycle design: air intake manifold demonstration project, *Journal of Cleaner Production*, 11, 2003, 61–77.
- [3] Siqueira, C.D.L.R., Kessler, M.P., De Araújo, L.A.R., Rodrigues, E.C., Three-dimensional Transient Simulation of an Intake Manifold using CFD Techniques, *SAE Technical Paper*, 2006, 0148-7191.
- [4] Ceviz, M., Intake plenum volume and its influence on the engine performance, cyclic variability and emissions, *Energy Conversion and Management*, 48 (3), 2007, 961-966.
- [5] Ceviz, M., Akın, M., Design of a new SI engine intake manifold with variable length plenum, *Energy Conversion and Management*, 51(11), 2010, 2239-2244.
- [6] Jemni, M.A., Kantchev, G., Abid, M.S., Influence of intake manifold design on in-cylinder flow and engine performances in a bus diesel engine converted to LPG gas fuelled, using CFD analyses and experimental investigations, *Energy* 36, 2011, 2701-2715.
- [7] Butt, Q.R., Bhatti, A.I., Mufti, M.R., Rizvi, M.A., Awan, I., Modeling and online parameter estimation of intake manifold in gasoline engines using sliding mode observer, *Simulation Modelling Practice and Theory*, 32, 2013, 138–154.
- [8] Vichi, G., Romani, L., Ferrari, L., Ferrara, G., Development of an engine variable geometry intake system for a Formula SAE application, *Energy Procedia*, 81, 2015, 930-941.
- [9] Manmadhachary, A., Kumar, M.S., Kumar, Y.R., Design&manufacturing of spiral intake manifold to improve Volumetric efficiency of injection diesel engine by AM process, *Materials Today: Proceedings*, 4, 2017, 1084–1090.
- [10] Giannakopoulos, G.K., Frouzakis, C.E., Boulouchos, K., Fischer, P.F., Tomboulides, A.G., Direct numerical simulation of the flow in the intake pipe of an internal combustion engine, *International Journal of Heat and Fluid Flow*, 68, 2017, 257–268.
- [11] Zhao, J., Xi, Q., Wang, S., Wang, S., Improving the partial-load fuel economy of 4-cylinder SI engines by combining variable valve timing and cylinder-deactivation through double intake manifolds, *Applied Thermal Engineering*, 141, 2018, 245–256.
- [12] Hall, C.M., Shaver, G.M., Chauvin, J., Petit, N., Control-oriented modelling of combustion phasing for a fuel-flexible spark-ignited engine with variable valve timing, *International Journal of Engine Research*, 13, 2012, 448-463.
- [13] Silva, E.A.A., Ochoa, A.A.V., Henriquez, J.R., Analysis and runners length optimization of the intake manifold of a 4-cylinder spark ignition engine, *Energy Conversion and Management*, 188, 2019, 310–320.
- [14] Sadeq, A.M., Bassiony, M.A., Elbashir, A.M., Ahmed, S.F., Khraisheh, M., Combustion and emissions of a diesel engine utilizing novel intake manifold designs and running on alternative fuels, *Fuel*, 255, 2019, 115769.
- [15] Souza, G.R.D., Pellegrini, C.D.C., Ferreira, S.L., Pau, F.S., Armas, O., Study of intake manifolds of an internal combustion engine: A new geometry based on experimental results and numerical simulations, *Thermal Science and Engineering Progress*, 9, 2019, 248–258.
- [16] Liu, G., Ruan, C., Li, Z., Huang, G., Zhou, Q., Qian, Y., Lu, X., Investigation of engine performance for alcohol/kerosene blends as in spark-ignition aviation piston engine, *Applied Energy*, 268, 2020, 114959.
- [17] Menzel, G., Och, S.H., Mariani, V.C., Moura, L.M., Domingues, E., Multi-objective optimization of the volumetric and thermal efficiencies applied to a multi-cylinder internal combustion engine, *Energy Conversion and Management*, 216, 2020, 112930.
- [18] Mariani, V.C., Och, S.H., Coelho, L.D.S., Domingues, E., Pressure prediction of a spark ignition single cylinder engine using optimized extreme learning machine models, *Applied Energy*, 249, 2019, 204-221.
- [19] Zhao, H., Zhao, N., Zhang, T., Wu, S., Ma, G., Yan, C., Ju, Y., Studies of multi-channel spark ignition of lean n-pentane/air mixtures in a spherical chamber, *Combustion and Flame*, 212, 2020, 337-344.
- [20] Och, S.H., Moura, L.M., Mariani, V.C., Coelho, L.D.S., Velásquez, J.A., Domingues, E., Volumetric efficiency optimization of a single-cylinder D.I. diesel engine using differential evolution algorithm, *Applied Thermal Engineering*, 108, 2016, 660-669.
- [21] Shi, C., Ji, C., Wang, S., Yang, J., Ma, Z., Xu, P., Assessment of spark-energy allocation and ignition environment on lean combustion in a twin-plug Wankel engine, *Energy Conversion and Management*, 209, 2020, 112597.
- [22] Gocmen, K., Soyhan, H.S., An intake manifold geometry for enhancement of pressure drop in a diesel engine, *Fuel*, 261, 2020, 116193.
- [23] Chalet, D., Mahe, A., Migaud, J., Hetet, J.F., A frequency modelling of the pressure waves in the inlet manifold of internal combustion engine, *Applied Energy*, 88, 2011, 2988-2994.
- [24] Hasankola, S.S.M., Shafaghat, R., Jahanian, O., Nikzadfar, K., An experimental investigation of the injection timing effect on the combustion phasing and emissions in reactivity-controlled compression ignition (RCCI) engine, *Journal of Thermal Analysis and Calorimetry*, 139, 2020, 2509–2516.
- [25] Boretti, A., Water injection in directly injected turbocharged spark ignition engines, *Applied Thermal Engineering*, 52(1), 2013, 62-68.
- [26] Bozza, F., De Bellis, V., Teodosio, L., Potentials of cooled EGR and water injection for knock resistance and fuel consumption improvements of gasoline engines, *Applied Energy*, 169, 2016, 112-125.
- [27] Vos, K.R., Shaver, G.M., Lu, X., Allen, C.M., Jr, J.M., Farrell, L., improving diesel engine efficiency at high speeds and loads through improved breathing via delayed intake valve closure timing, *International Journal of Engine Research*, 20, 2019, 194-202.
- [28] Gong, C., Yu, J., Wang, K., Liu, J., Huang, W., Si, X., Wei, F., Liu, F., Han, Y., Numerical study of plasma produced ozone assisted combustion in a direct injection spark ignition methanol engine, *Energy*, 153, 2018, 1028-1037.
- [29] Trindade, W.R.D.S., Santos, R.G.D., 1D modeling of SI engine using n-butanol as fuel: Adjust of fuel properties and comparison between measurements and simulation, *Energy Conversion and Management*, 157, 2018, 224-238.
- [30] Ghazal, O.H., Combustion analysis of hydrogen-diesel dual fuel engine with water injection technique, *Case Studies in Thermal Engineering*, 13,







2019, 100380.


[31] Tuchler, S., Dimitriou, P., On the capabilities and limitations of predictive, multi-zone combustion models for hydrogen diesel dual fuel operation, *International Journal of Hydrogen Energy*, 44, 2019, 18517–18531.

## ORCID iD

Mostafa Khajezadeh Roodi  <https://orcid.org/0000-0001-5063-355X>

Ali Jalali  <https://orcid.org/0000-0001-7897-0769>

Ali Hedayati  <https://orcid.org/0000-0002-6881-927X>

Amin Amiri Delouei  <https://orcid.org/0000-0001-7414-4195>



© 2021 Shahid Chamran University of Ahvaz, Ahvaz, Iran. This article is an open access article distributed under the terms and conditions of the Creative Commons Attribution-NonCommercial 4.0 International (CC BY-NC 4.0 license) (<http://creativecommons.org/licenses/by-nc/4.0/>).

**How to cite this article:** Roodi M.K., Jalali A., Hedayati A., Delouei A.A. Optimization of Spark Ignition Engine Performance Using a New Double Intake Manifold: Experimental and numerical analysis, *J. Appl. Comput. Mech.*, 9(1), 2023, 1–14.  
<https://doi.org/10.22055/JACM.2020.34234.2365>

**Publisher's Note** Shahid Chamran University of Ahvaz remains neutral with regard to jurisdictional claims in published maps and institutional affiliations.

